Available online at www.sciencedirect.com
ScienceDirect
Journal of Power Sources 174 (2007) 949–953
JOURNAL OF POWER SOURCES
www.elsevier.com/locate/jpowsour

Short communication

Effect of particle size on $LiMnPO_4$ cathodes

Thierry Drezen [a], Nam-Hee Kwon [a], Paul Bowen [b], Ivo Teerlinck [c], Motoshi Isono [d], Ivan Exnar [a,*]

[a] *High Power Lithium (HPL), Scientific Park B (PSE-B), Swiss Federal Institute of Technology, Lausanne, Switzerland*
[b] *Laboratoire de Technique des Poudres (LTP), Institut des Matériaux, Faculté des Sciences et Techniques de l'ingénieur, Ecole, Polytechnique Fédérale de Lausanne, Lausanne, Switzerland*
[c] *Toyota Motor Europe NV/SA, Hoge Wei 33, B-1930 Zaventem, Belgium*
[d] *Material Engineering Division, Toyota Motor Corporation, Toyota-cho, Toyota-shi, Aichi 471-8571, Japan*

Available online 30 June 2007

Abstract

$LiMnPO_4$ was synthesized using a sol–gel method and tested as a cathode material for lithium ion batteries. After calcination at temperatures between 520 and 600 °C, primary particle sizes in the range of 140–220 nm were achieved. Subsequent dry ball milling reduced the primary particle diameters from 130 to 90 nm, depending on time of ball milling. Reversible capacities of 156 mAh g^{-1} at *C*/100 and 134 mAh g^{-1} at *C*/10 were measured. At 92% and 79% of the theoretical values, respectively, these are the highest values reported to date for this material. At faster charging rates, the electrochemical performance was found to be improved when smaller $LiMnPO_4$ particles were used.

Keywords: $LiMnPO_4$; Sol–gel synthesis; Lithium ion battery; Cathode material; Specific energy storage; Rate capacity and particle size effects

1. Introduction

Lithium transition-metal (*ortho*) phosphates have recently attracted attention as potential Li-ion battery cathode materials due to their lower toxicity, lower cost and better chemical and thermal stability, when compared to the currently used $LiCoO_2$. The three-dimensional framework of an olivine is stabilized by the strong covalent bonds between oxygen ions and the P^{5+} resulting in PO_4^{3-} tetrahedral polyanions [1]. As a consequence, olivine lithium metal phosphate materials do not undergo a structural re-arrangement during lithiation and de-lithiation. This means that they do not experience the capacity fade during cycling suffered by lithium transition metal oxides such as $LiCoO_2$, $LiNiO_2$, $LiMnO_2$ and $LiMn_2O_4$. This is attributed to structural rearrangements caused during lithiation and de-lithiation.

Lithium manganese phosphate has a redox potential of 4.1 V versus Li^+/Li [1,2], which is considered to be the maximum limit accessible to most liquid electrolytes. Unfortunately, $LiMnPO_4$ has a low intrinsic electronic and ionic conductivity and hence a poor discharge rate capability. The electrochemical performance is especially poor at high current densities, this is assigned to the slow lithium diffusion kinetics within the grains and the low intrinsic electronic conductivity [3,4]. An approach to improve the rate performance of the olivine material is to minimize the particle size [5,6]. This reduces the diffusion path length for lithium ions in the cathode material and also creates a large contact area with conductive additives such as carbon [7–9].

Delacourt et al. [10] synthesized 100 nm diameter particles of $LiMnPO_4$ by precipitation, which enhanced the reversible capacity to 70 mAh g^{-1} at *C*/20 from only 35 mAh g^{-1} for 1 μm diameter particles. Yonemura et al. [4] reached 150 mAh g^{-1} of discharge capacity at *C*/100 with small particles, close to the theoretical capacity of 170 mAh g^{-1}. Thus, it is evident that particle size is critical in determining useful lithium capacity and charge/discharge rates [11–14]. So far, the production of mesoparticulate $LiMPO_4$ (M = Fe, Mn) remains a challenge and only a few groups have successfully produced materials of appropriate dimensions to yield the desired electrochemical performance in lithium ion batteries. The sol–gel synthesis technique offers a convenient means of producing particles of small size from homogeneous mixing of reagents on an atomic scale. In this paper we report the electrochemical performance

* Corresponding author.
E-mail address: i.exnar@highpowerlithium.com (I. Exnar).

0378-7753/$ – see front matter © 2007 Elsevier B.V. All rights reserved.
doi:10.1016/j.jpowsour.2007.06.203

of sol–gel prepared $LiMnPO_4$ with various particle sizes at low and high current densities.

2. Experimental

$LiMnPO_4$ powder was prepared by a sol–gel method using lithium acetate dihydrate, manganese acetate tetrahydrate and ammonium dihydrogen phosphate as precursors. The starting materials were dissolved in distilled water at room temperature and glycolic acid was used as a chelating agent. The pH of the resulting solution was adjusted to below 4 by the addition of concentrated HNO_3. This solution was then heated to 60–75 °C to obtain a gel and the latter was dried overnight at 120 °C before being heated for 5 h at 350 °C under air. The powder as produced was then calcined at different incremental temperatures (450–800 °C) for 3 h in air.

The crystal structure of the resulting powder was examined by X-ray diffraction (XRD) using Cu Kα radiation and a 2θ step of 0.04°. The surface area of the samples before and after ball milling was measured by nitrogen adsorption using the Brunauer–Emmett–Teller (BET) model. Particle size distribution was measured by laser diffraction (Malvern Mastersizer). The morphology and the particle size were investigated with field-emission scanning electron microscopy (FESEM, Philips XL30 FEG). After calcination, the $LiMnPO_4$ powder was dry ball-milled (RETSCH PM 4000) with 20 wt% of acetylene black for 4 h to obtain a carbon–$LiMnPO_4$ (C–$LiMnPO_4$) composite. Electrodes for electrochemical testing were prepared by tape casting a *N*-methyl pyrrolidone (NMP) slurry of the C–$LiMnPO_4$ composite (90 wt%) with poly(vinylidene fluoride) (PVdF) binder (5 wt%) and acetylene black (5 wt%) on an aluminum current collector. After drying at 120 °C under vacuum, the electrodes were compressed into 23 mm Ø disks with a thickness of 27–41 μm, the active material loading being 1.45–3.7 mg cm^{-2}. The cells were assembled in Swagelok™ fittings using Li metal foil as the counter electrode with a microporous polymer separator (Celgard 2400™) and liquid electrolyte mixtures containing 1M $LiPF_6$ in a solvent mixture of propylene carbonate (PC), ethlylene carbonate (EC) and dimethyl carbonate (DMC) (1:1:3 by volume). The electrochemical properties of $LiMnPO_4$ electrodes were measured by galvanostatic charge/discharge and cyclic voltammetry using an Arbin BT 2000 electrochemical measurement system.

3. Results

The crystal phase of our samples was identified from the powder XRD measurements to be $LiMnPO_4$ with an ordered olivine structure indexed by orthorhombic Pnmb powder prepared with an orthorhombic phase. XRD data for samples synthesized at different calcination reaction temperatures is shown in Fig. 1. The olivine phase was formed at a temperature as low as 350 °C even though the peak intensity was very low. The peak intensity increased with reaction temperature, indicating improved crystallization and particle growth. The mean particle size calculated from BET data, D_{BET} (shown in Fig. 2), demonstrates

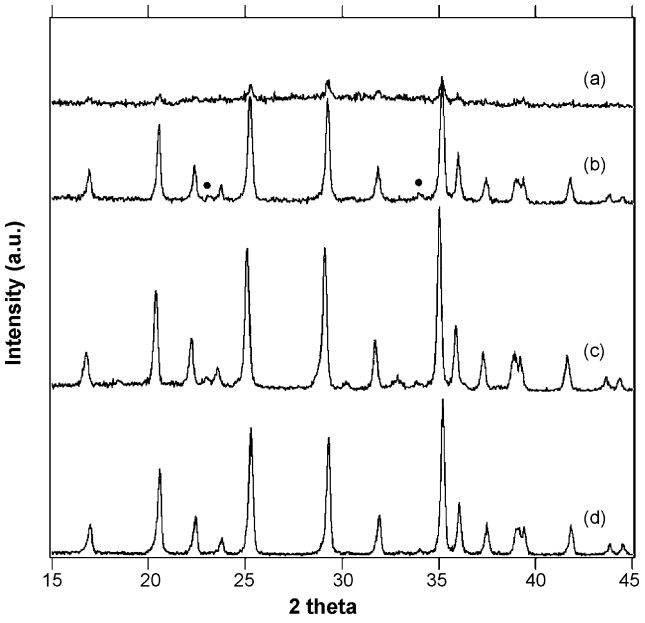

Fig. 1. XRD diffraction patterns of the powders annealed at (a) 350 °C for 5 h, (b) 450 °C for 3 h, (c) 520 °C for 3 h and (d) 570 °C for 3 h. The ● labeled peaks indicate an impurity phase (Li_3PO_4).

that the average particle size increases dramatically between 600 and 800 °C. The powders calcinated at temperatures below 600 °C maintain a smaller D_{BET}, of under 200 nm and have a well-crystallized olivine phase of $LiMnPO_4$. The powders showed a certain degree of agglomeration with a median volume diameter D_{v50} from the laser diffraction of around 4 μm.

The $LiMnPO_4$ powder was dry ball-milled with 20 wt% of acetylene black for 4 h to obtain a carbon–$LiMnPO_4$ (C–$LiMnPO_4$) composite. During ball milling the primary particle size was reduced. For a compound calcined at 600 °C with an initial specific surface area of 8.0 m^2 g^{-1}, 3 h of ball milling increased the BET value to 18.5 m^2 g^{-1} (Fig. 4). A particle size distribution (PSD) analysis shows an agglomeration of our material. The as-calcined $LiMnPO_4$ gave a mono-modal PSD with

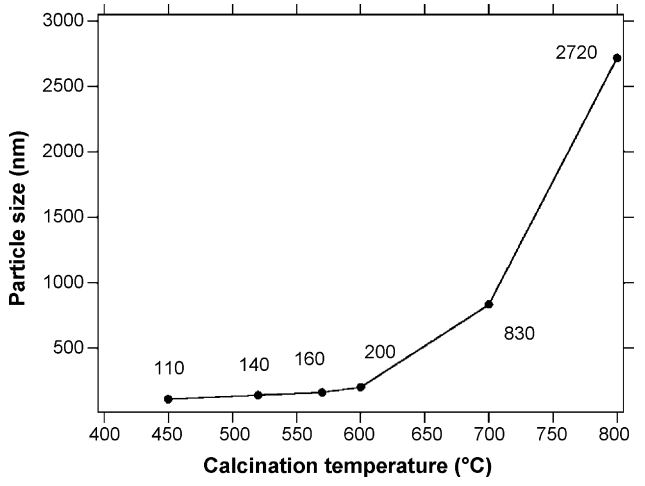

Fig. 2. Variation in primary particle size, D_{BET}, of $LiMnPO_4$ as a function of annealing temperature.

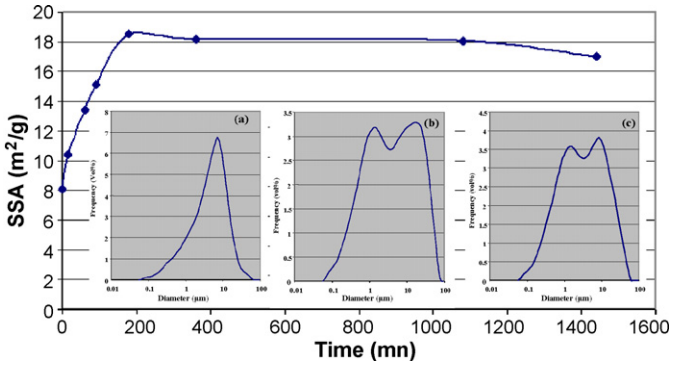

Fig. 3. Variation of the specific surface area of a $LiMnPO_4$ calcined at 600 °C and volume particle size distribution (a) of the as-calcined $LiMnPO_4$, (b) after 3 h of ball milling and (c) after 24 h of ball milling.

agglomerates of 4 μm (D_{v50}). PSDs of $LiMnPO_4$ with milling times from 15 min to 24 h showed bi-modal size distribution. The mean diameter decreased until 3 h of ball milling but then increased with further milling time (insets Fig. 3). This indicates that the primary particles of about 100 nm diameter are aggregated giving a D_{v50} of 2.5 μm after 3 h milling. The primary particle size is decreased by planetary ball milling but the agglomeration becomes more marked as ball milling time increases.

SEM was applied to investigate the particle size and the morphology of materials calcinated at 520, 600 and 700 °C. As shown in Fig. 4(a), the SEM images of powders calcinated at 520 °C, show small and uniform particle dimensions. In Fig. 4(c) particles synthesized at 600 °C are clearly larger than Fig. 4(a) and the particle size distribution is broad.

Reversible capacities of the C–$LiMnPO_4$ composite powders were measured at *C*/10 and are shown in the form of cycling tests in Fig. 4. The sample calcinated at 520 °C demonstrated the highest capacity of 134 mAh g^{-1} at *C*/10. The results demonstrate that the specific capacities decrease as the particle size increases.

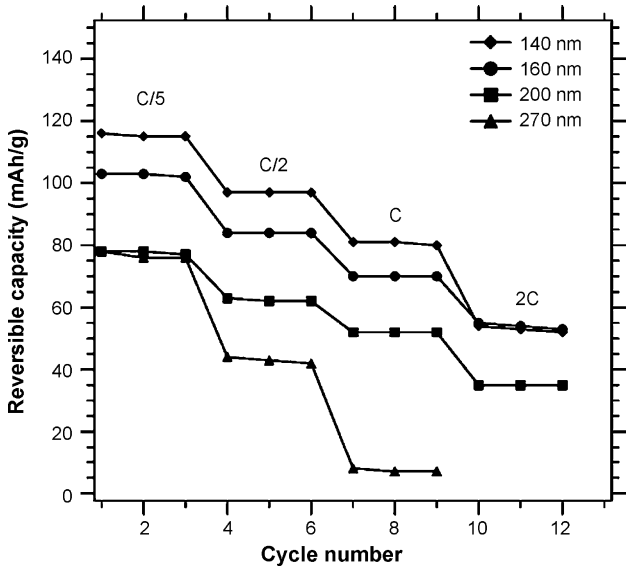

Fig. 5. Rate capabilities for different particle sizes of $LiMnPO_4$.

Rate capabilities for four different particle sizes are shown in Fig. 5. One hundred and forty nanometer particles reached a reversible capacity of 116 mAh g^{-1} at *C*/5 (68% of the theoretical capacity). At 1*C*, the reversible capacities for the 140 and 270 nm diameter $LiMnPO_4$ particles are 81 and 7 mAh g^{-1}, respectively. Increasing particle size impacts rapidly on the absolute and reversible lithium capacities of $LiMnPO_4$. This can be rationalized by a simple consideration of the lithium insertion and extraction kinetics and the poor electrical conductivity of the active phase. As the particle size increases, lithium diffusion becomes increasingly difficult due to both the diffusion limitation of Li^+ within a single large particle and the difficulty of electron transport through the bulk of this material.

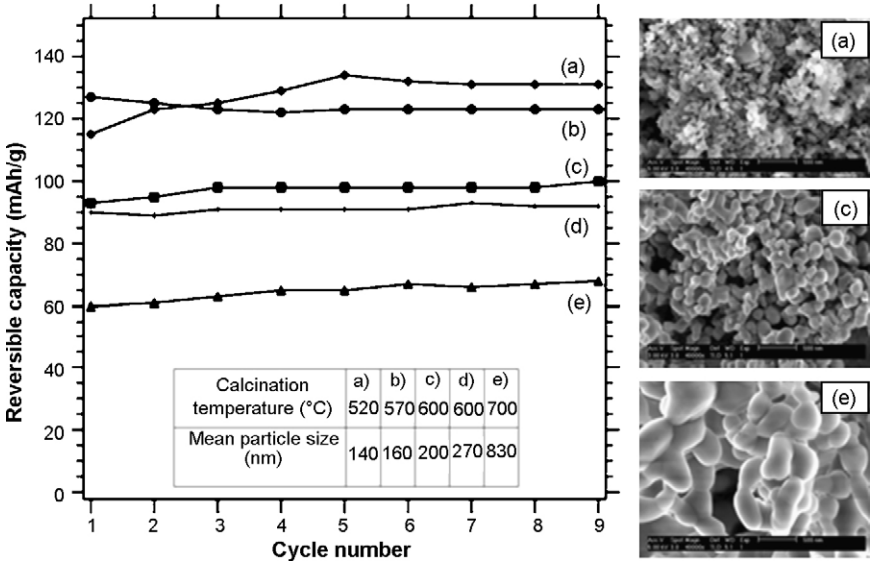

Fig. 4. The cycling performance at 0.1*C* of $LiMnPO_4$ prepared via sol–gel using different calcination temperatures (a) 520 °C, (b) 570 °C, (c) 600 °C, (d) 600 °C and (e) 700 °C and SEM images of $LiMnPO_4$ annealed at (a) 520 °C, (c) 600 °C and (e) 700 °C.

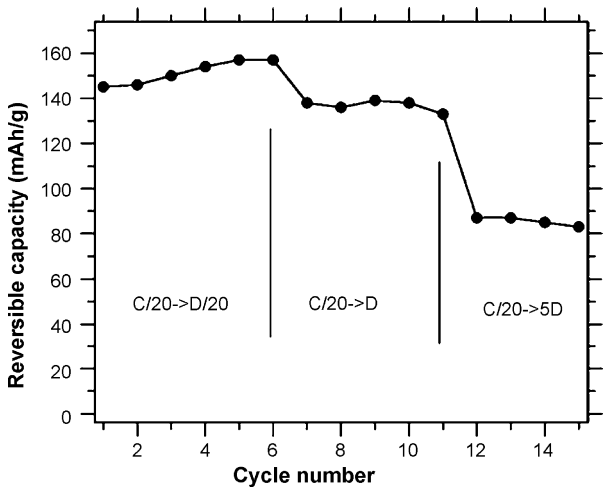

Fig. 6. The reversible capacities at various discharging rates in the same condition of charging rate of *C*/20. Charging and discharging rates were calculated from the nominal capacity of 150 mAh g^{-1}.

Fig. 6 shows 150–160 mAh g^{-1} of reversible capacity at *D*/20 after charging rate of *C*/20. Subsequently the material was charged again at *C*/20 rate and it still obtained 120–130 mAh g^{-1} of reversible capacity at 1*D*. At 5*D*, 65–85 mAh g^{-1} of discharge capacity was observed. The charge and discharge rate was calculated from a maximum practical capacity of 150 mAh g^{-1}. Therefore, we reached the maximum capacity even at *C*/20 and *D*/20 instead of *C*/100 and *D*/100. And the material achieved 87% of the maximum capacity at 1*D*.

4. Discussion

It is suggested that to improve the electrochemical performance of olivine electrodes, it is necessary to improve both ion and electron transport. Improvement in ion transport is achieved by decreasing the particle size and ensuring a narrow size distribution [13,15]. Improvement in electron transport is achieved by carbon coating the cathode material and by adding carbon to the cathode.

Predictably, increasing the calcination reaction temperature results in the formation of larger $LiMnPO_4$ primary particles. We demonstrate that increasing primary particle size impacts rapidly on the absolute and reversible lithium capacities of $LiMnPO_4$. This can be rationalized by a simple consideration of the lithium insertion and extraction kinetics and the poor electrical conductivity of the active phase. As the primary particle size increases, lithium diffusion becomes increasingly difficult due to both the diffusion limitation of Li^+ within a single large particle and the difficulty of electron transport through the bulk of this material. When the primary particle size is large, it will take a much longer time for lithium ions to diffuse into the core of the particle to make a single homogeneous phase of $LiMn^{2+}PO_4$ or $Mn^{3+}PO_4$. The important observation from this work is to recognize that the mesoparticulate uniform $LiMnPO_4$ materials synthesized at lower reaction temperatures allow for shorter lithium ion diffusion lengths within a single particle.

In addition, we used a high-energy planetary ball milling to make a homogeneous mixture of the active $LiMnPO_4$ material and carbon and also to make a uniform carbon network connection between carbon particles.

The combination of small primary particle size and carbon coating results in enhanced specific capacities beyond 92% of the theoretical capacity (156 mAh g^{-1} at *C*/100). The performance of 116 mAh g^{-1} at *C*/5 exceeds the best previously reported values of 70 mAh g^{-1} at *C*/20 [10] and 135 mAh g^{-1} at *C*/25 [4].

5. Conclusions

Near optimal charge/discharge capacity performance has been obtained from mesoparticulate $LiMnPO_4$ cathode material in lithium ion batteries. The primary particle size for low conductivity $LiMnPO_4$ is crucial to the electrochemical performance. A relatively low reaction temperature produces well-crystallized small powders (140–160 nm) with a uniform particle size and morphology. These materials achieved excellent charge/discharge kinetics of lithium ions. Once coated with carbon via ball milling, electrodes produced from these materials demonstrate capacities, close to the theoretical limit. The results obtained are clearly superior to literature data on $LiMnPO_4$, confirming that the sol–gel route provides a suitable preparation method.

Acknowledgements

The authors thank Centre Interdisciplinaire de Microscopie Electronique (CIME) for the opportunity to access SEM apparatus. We also thank P. Comte and M. Crouzet for BET measurements and electrochemical measurements, respectively.

References

[1] A.K. Padhi, K.S. Nanjundaswamy, J.B. Goodenough, J. Electrochem. Soc. 144 (4) (1997) 1188–1194.
[2] A. Yamada, S.C. Chung, J. Electrochem. Soc. 148 (8) (2001) A960–A967.
[3] C. Delacourt, L. Laffont, R. Bouchet, C. Wurm, J.B. Leriche, M. Morcrette, J.M. Tarascon, C. Masquelier, J. Electrochem. Soc. 152 (5) (2005) A913–A921.
[4] M. Yonemura, A. Yamada, Y. Takei, N. Sonoyama, R. Kanno, J. Electrochem. Soc. 151 (9) (2004) A1352–A1356.
[5] A. Yamada, S.C. Chung, K. Hinokuma, J. Electrochem. Soc. 148 (3) (2001) A224–A229.
[6] P.P. Prosini, M. Carewska, S. Scaccia, P. Wisniewski, M. Pasquali, Electrochim. Acta 48 (28) (2003) 4205–4211.
[7] C.H. Mi, X.B. Zhao, G.S. Cao, J.P. Tu, J. Electrochem. Soc. 152 (3) (2005) A483–A487.
[8] S.T. Myung, S. Komaba, N. Hirosaki, H. Yashiro, N. Kumagai, Electrochim. Acta 49 (24) (2004) 4213–4222.
[9] H. Huang, S.C. Yin, L.F. Nazar, Electrochem. Solid-State Lett. 4 (10) (2001) A170–A172.
[10] C. Delacourt, P. Poizot, M. Morcrette, J.M. Tarascon, C. Masquelier, Chem. Mater. 16 (1) (2004) 93–99.
[11] G.T.K. Fey, R.F. Shiu, V. Subramanian, C.L. Chen, Solid State Ionics 148 (3–4) (2002) 291–298.

[12] Y.Q. Hu, M.M. Doeff, R. Kostecki, R. Finones, J. Electrochem. Soc. 151 (8) (2004) A1279–A1285.
[13] P.P. Prosini, M. Lisi, D. Zane, M. Pasquali, Solid-State Ionics 148 (1–2) (2002) 45–51.
[14] Nam-Hee Kwon, Thierry Drezen, Ivan Exnar, Ivo Teerlinck, Motoshi Isono, Graetzel Michael, Electrochem. Solid-State Lett. 9 (6) (2006) A277–A280.
[15] V. Srinivasan, J. Newman, J. Electrochem. Soc. 151 (10) (2004) A1517–A1529.